
Article:
Díaz-Canul, F., Aguilar, J.O. orcid.org/0000-0001-9325-0591, Rosado-Hau, N. et al. (2 more authors) (2025) Design of low-power vertical-axis wind turbine based on parametric method. Wind, 5 (4). p. 35. ISSN: 2674-032X

https://doi.org/10.3390/wind5040035

---

wind

MDPI

Article

Design of Low-Power Vertical-Axis Wind Turbine Based on Parametric Method

F. Díaz-Canul [1], J. O. Aguilar [1,*], N. Rosado-Hau [2], E. Simá [3] and O. A. Jaramillo [4]

[1] Science and Technology Department, Universidad Autónoma del Estado de Quintana Roo, Boulevard Bahía s/n col del Bosque, Chetumal 77019, Quintana Roo, Mexico; 1518010@uqroo.edu.mx
[2] Multidisciplinary Engineering Education, University of Sheffield, Sheffield S10 2TN, UK; n.rosadohau@sheffield.ac.uk
[3] Department of Mechanical Engineering, Tecnológico Nacional de México, Centro Nacional de Investigación y Desarrollo Tecnológico (CENIDET-TecNM), Cuernavaca 62493, Morelos, Mexico; efrain.sm@cenidet.tecnm.mx
[4] Instituto de Energías Renovables, Universidad Nacional Autónoma de México, Priv. Xochicalco s/n, Temixco 62588, Morelos, Mexico; ojs@ier.unam.mx
* Correspondence: ovidio@uqroo.edu.mx; Tel.: +52-9831142829

Abstract

The parametric design of a low-power (<1 kW) H-type vertical-axis wind turbine tailored to the wind conditions of the Yucatán Peninsula is presented. Nine airfoils were evaluated using the Double Multiple Streamtube method and Qblade Lifting-Line Theory numerical simulations, considering variations in solidity (σ = 0.20–0.30), aspect ratio ($A_r = H/R$ = 2.6–3.0), number of blades (2–5), and a swept-area constraint of 4 m^2. The parametric study shows that fewer blades increase Cp, although a three-blade rotor improves start-up torque, vibration mitigation, and load smoothing. The recommended configuration—three blades, A_r = 2.6, σ = 0.30 and S1046 (or NACA 0018) operated near λ ≈ 3.75—balances efficiency and start-up performance. For the representative mean wind velocity of 5 m/s, typical of the Yucatán Peninsula, the VAWT achieves a maximum output of 136 W at 220 rpm. Under higher-wind conditions observed in specific sites within the region, the predicted maximum output increases to 932 W at 380 rpm.

Keywords: DMS; QLLT; Qblade; vertical axis wind turbine; VAWT design

Academic Editor: Francesco Castellani

Received: 8 October 2025
Revised: 13 November 2025
Accepted: 25 November 2025
Published: 10 December 2025

Citation: Díaz-Canul, F.; Aguilar, J.O.; Rosado-Hau, N.; Simá, E.; Jaramillo, O.A. Design of Low-Power Vertical-Axis Wind Turbine Based on Parametric Method. *Wind* **2025**, *5*, 35. https://doi.org/10.3390/wind5040035

1. Introduction

British Petroleum's energy outlook for 2024 predicts that the current zero-emissions capacity of solar and wind energy will grow approximately eight- and fourteen-fold, respectively, by 2050. For this reason, the continued development of better technology for harnessing these energies, in this case wind energy, is crucial. Vertical axis wind turbines (VAWTs) have an advantage over horizontal axis wind turbines (HAWTs) in that they are omnidirectional without requiring a directional control system, are more aesthetically pleasing, are more efficient in turbulent environments, and produce less noise. Furthermore, they operate at much lower wind speeds than horizontal axis turbines. However, in most cases, an initial drive system is required. Darrieus-type turbines are particularly popular owing to their stable power coefficient, high reliability, and low noise emissions [1].

According to several authors [2–4] the main design parameters for a Darrieus-type vertical axis wind turbine are (i) solidity (σ); (ii) height/diameter ratio (ϕ = H//D); (iii) chord/diameter ratio ($\xi = c/D$); (iv) rotor swept area (A); (v) airfoil; and (vi) support structure dimensions. These parameters must be optimized to obtain the maximum

amount of energy from the wind using a VAWT or HAWT. It is also necessary to choose the appropriate airfoil for the blades based on the wind resources at the site where they are to be installed. Several studies have carried out the optimization of airfoils [5–7], to reduce self-starting torque. Wind turbine robustness is another important factor to consider. Ref. [8] found that the optimal solidity can be determined through aerodynamic analysis. The number of turbine blades depends on several important parameters, such as the uniformity of power output, turbine loads and vibrations, and turbine cost and performance. On the other hand, ref. [9] mentions that it is preferable to use high-solidity variable-pitch blades when self-starting torque is required, as this type of blade is capable of producing more torque at high solidity values. In addition, σ is closely related to the number of rotor blades; the greater the number of blades, the greater the solidity. However, ref. [10] mentions that there is a trade-off between the power coefficient (Cp) of a VAWT and solidity, since (Cp) increases as σ decreases. Therefore, a wind turbine design that minimizes the negative impact of the main design parameters on the wind turbine's power coefficient is extremely important.

In Mexico, great academic efforts have been made to develop technology for harnessing wind energy, mainly through graduate research. It is important to mention that in Mexico there are no national developments regarding low-power vertical axis wind turbines. Low-power wind turbines have been designed for specific regions, i.e., according to the wind potential of the area where they are to be installed (average annual wind speed). Low-power vertical- and horizontal-axis wind turbine designs have been proposed, such as those developed by [11–14]. The novelty of this research lies in providing a methodology based on parametric study for the aerodynamic design of low-power vertical-axis wind turbines using an open-source tool. Although it focuses on wind resources in the Yucatan Peninsula, its use can be extended to different locations.

This work aims to develop the aerodynamic design of a VAWT, which consists of a parametric design of a low-power (<1 kW) H-type vertical axis wind turbine using free available computational tools, such as QBlade (v0.96), which employs the DMS (Double Multiple Stream model) and QLLT (QBlade Lifting Line Theory) methods instead of CFD commercial software. The selection of the electric generator and the structural resistance to wind loads are not considered. The parametric design considers the variation in blade height (H), airfoil chord (c), radius (r), and rotor solidity (σ), as well as the number of blades (N) and the H/R ratio. Note that the methodology for designing the VAWT rotor was validated with the experimental work done by [15] and reported in [16].

2. Framework

2.1. VAWT Aerodynamics

The theoretical formulation for analyzing VAWTs differs greatly from that of HAWTs simply because of their orientation in relation to the wind. This difference makes analyzing VAWTs a more complex task, despite the mathematical expressions used to describe them being based on the same assumptions.

2.2. VAWT Velocities

Velocities

The study of the velocities acting on a VAWT requires analysis in two areas: when the wind enters the rotor (upstream) and when it leaves it (downstream). These velocities differ in magnitude. In the downstream area, the wind has already interacted with the rotor blades, and its magnitude is reduced, converting part of the wind's kinetic energy into mechanical energy. The relative airflow velocity (W) with which lift and drag forces are obtained is determined from the chord velocity (v_c) and normal velocity (v_n), which

are shown in Figure 1. The chord velocity is the sum of the tangential velocity due to the rotation of the rotor ($R \times \omega$) and the component of the axial velocity (v_a) in the tangential direction, as expressed in Equation (2) [17].

$$W = \sqrt{V_c^2 + V_n^2} \tag{1}$$

For velocity analysis, a wind flow incident in an axial direction is considered. The chord velocity V_c can be expressed as follows:

$$V_c = R\omega + V_a cos\theta \tag{2}$$

where V_a is the axial velocity (induced velocity), ω is the rotational speed, R is the rotor radius, and θ is the azimuth angle. Similarly, the normal velocity V_n, which is the component of the axial velocity of the air flow in the normal direction (towards the center of the rotor), is expressed as:

$$V_n = V_a sin\theta \tag{3}$$

The angle of attack is determined from (V_c) and (V_n) as follows:

$$\alpha = tan^{-1}\left(\frac{V_n}{V_c}\right) \tag{4}$$

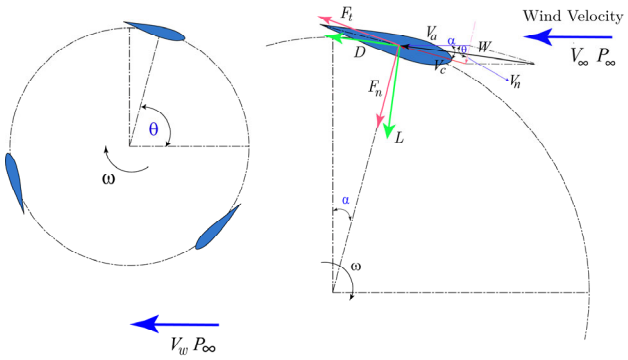

Figure 1. Flow velocities of straight-blades Darrieus-type VAWT.

2.3. Forces Acting on the VAWT

Figure 2 shows the drag, and lift forces an airfoil, and its tangential and normal components are subject to. These forces are obtained by totaling the tangential and normal components of the lift (L) and drag (D) forces and are expressed as [17]:

$$F_t = L\, sin\alpha - D\, cos\alpha \tag{5}$$

$$F_n = L\, cos\alpha - D\, sin\alpha \tag{6}$$

The tangential force provides torque for power generation in the VAWT, and the normal force exerts structural load on the VAWT tower. Lift and drag forces are determined as follows:

$$F_L = \frac{1}{2} C_L \rho C H W^2 \tag{7}$$

$$F_D = \frac{1}{2} C_D \rho C H W^2 \tag{8}$$

where the air density is ρ, C is the airfoil chord, and H is the wind turbine height.

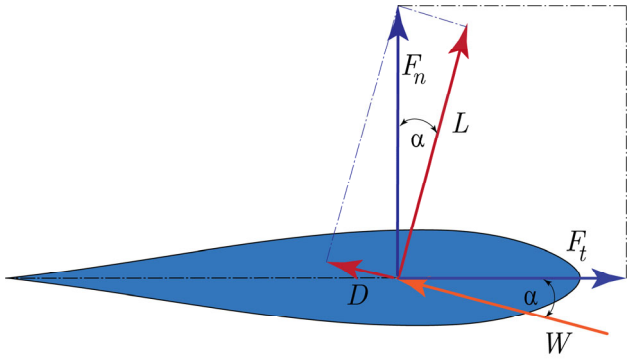

Figure 2. Free-body diagram of a wind turbine airfoil.

2.4. Torque

As mentioned above, the tangential force is what provides torque to the wind turbine and is a function of the azimuth angle θ. Therefore, to determine the average tangential force on the wind turbine, it must be evaluated throughout one revolution (2π) according to the following expression:

The torque generated by a VAWT is the product of the average tangential force (F_{tav}) of each blade (N) times the rotor radius (R) and can be obtained from the following equation:

$$T = NF_{t_{av}}R \tag{9}$$

Finally, the power of the wind turbine is defined as the product of the torque (T) times its rotational speed (ω), and is determined as follows:

$$P = T{\cdot}\omega \tag{10}$$

3. Development

This section presents the development of the DMS and QLLT models for rotor and wind turbine design implemented in the QBlade software. It also describes the selection and evaluation of the airfoils used, as well as that of the wind turbine topology and its aerodynamic performance.

3.1. Airfoil Selection and Evaluation

Airfoil selection is a fundamental step in VAWT design. Airfoils were originally designed for aeronautical applications [18], inspired by the shape of bird wings. Over time, designs evolved into symmetrical profiles with a raindrop-like silhouette and asymmetrical profiles optimized for aircraft flight conditions. Because of this, early VAWT designs used these profiles. However, this had several disadvantages, as the optimal operating conditions for which the first aerodynamic profiles were designed do not correspond to the operating conditions of a low-power VAWT. Therefore, the use of these airfoils for VAWT design does not ensure optimal efficiency under typical operating conditions. Efforts have been made to design aerodynamic profiles specifically for optimal efficiency under wind turbine operating conditions [19–21]. These profiles offer superior performance over a wider range of attack angles, critical for wind turbine start-up, where the greatest variation in angle of attack occurs.

Nine aerodynamic profiles were selected for the wind turbine design, three based on their aerodynamic performance reported in the literature and six based on their similarity to the first three (two for each airfoil). The airfoils were evaluated using the DMS method, which is a low-fidelity, streamtube-based model that runs fast and suits early VAWT design. This model is used to determine the most suitable configuration for the VAWT design, using

the same low-power VAWT configuration as described in Table 1 and shown in Figure 3. The parameters described were determined following the recommendations made in [21].

Table 1. Setting parameters for aerodynamic analysis of airfoils.

Parameter	Value
Height (m)	2.6
Chord (m)	0.1
Radius (m)	1
Solidity (-)	0.3
Number of blades	3
H/R ratio	2.6

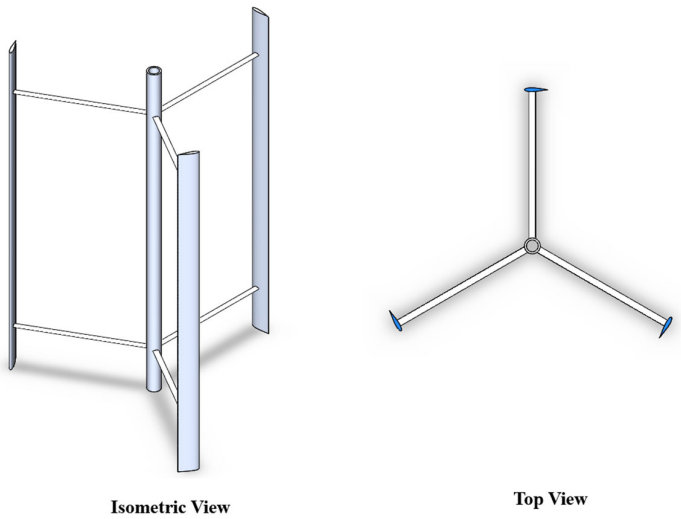

Figure 3. Different views of the vertical axis wind turbine (VAWT) used for airfoil evaluation.

The geometry of the six symmetrical (NACA 0021, S1046, Joukovsky 21, NACA 0018, Trainer 60, and Eppler 479) and three asymmetrical (DU 06-W-200, NASA SC(s) 0518, and NREL's S833) airfoils is shown in Figure 4. Those shown in the first row were chosen based on the performance reported in the literature by [19] (DU 06-W-200) and [21] (NACA 0021 y S1046). Airfoils like these three are shown in rows two and three.

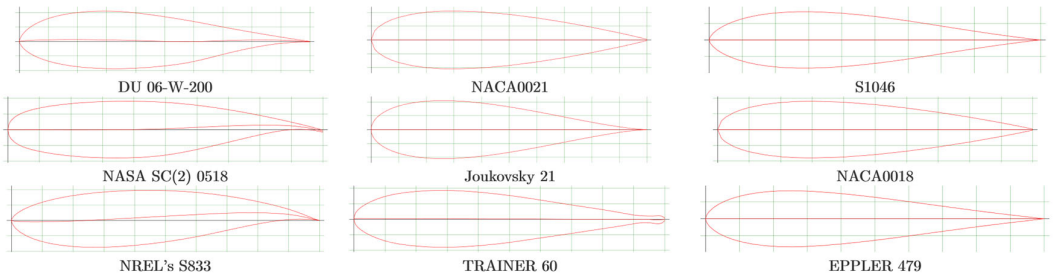

Figure 4. Airfoils selected for performance evaluation.

3.1.1. NACA 0021

The NACA 0021 is a symmetric airfoil that has been extensively studied for use in VAWTs. An important reason behind this is that it forms part of the family of symmetric 4-digit NACA airfoils, which have been studied and characterized in various experimental tests and CFD analyses, providing designers with greater certainty for sizing and predicting their aerodynamic behavior. Using XFoil (v6.99) software, aerodynamic performance was analyzed for four different Reynolds numbers (*Re*) (50×10^3, 100×10^3, 200×10^3 and

500 × 10^3). Figure 5 shows the lift coefficient as a function of the angle of attack (α) for this aerodynamic profile, in which linear behavior is observed for values between 0° and 8° for *Re* values greater than 100 × 10^3.

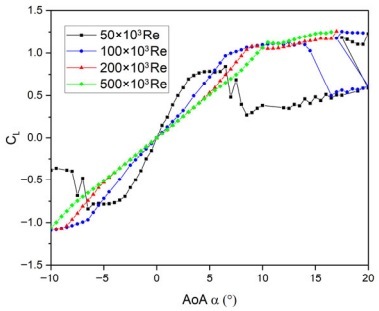

Figure 5. Lift coefficient (C_L) vs. angle of attack (α) for the NACA 0021 airfoil.

However, the curve for *Re* = 50 × 10^3 shows a very abrupt drop in performance, and therefore, it is essential to keep *Re* as high as possible when designing low-power VAWTs, as low wind speeds cause Re to fall below 100 × 10^3 for small rotors, as mentioned by [2]. This condition is critical for the proper performance of an aerodynamic profile. Figure 6 shows the drag coefficient (C_D) vs. angle of attack (α) for the same *Re* values. It can be seen that the C_D remains unchanged from −5° to 7°, increasing abruptly from 7° for a *Re* of 50 × 10^3. The Joukovsky 21 and Trainer 60 airfoils share geometric similarities with the NACA 0021.

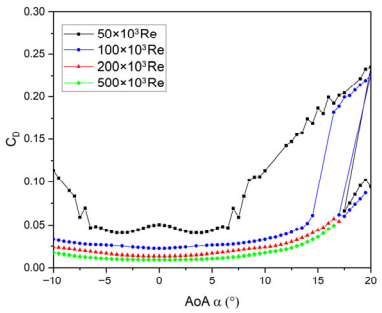

Figure 6. Drag coefficient (C_D) vs. angle of attack (α) for the NACA 0021 airfoil.

3.1.2. S1046

The S1046 is part of the family of airfoils designed by NREL for wind turbines. It performed well in tests conducted by [21], where it obtained a power coefficient of 0.4051. Figure 7 shows the lift coefficient behavior of this profile for different *Re* values. Linear behavior is observed for values between 0° and 10° for *Re* greater than 100 × 10^3. However, as with the NACA 0021 profile, the curve for *Re* = 50 × 10^3 shows a sharp drop in performance. Airfoils like S1046 identified by airfoil tools are NACA 0018 and Eppler 479. On the other hand, the C_D shows stable and reduced behavior from −4° to 4° for the four *Re* values, increasing outside that range. Figure 8 shows the C_D vs. α for this airfoil.

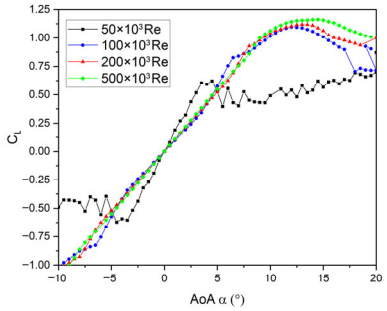

Figure 7. Lift coefficient (C_L) vs. angle of attack (α) for the S1046 airfoil.

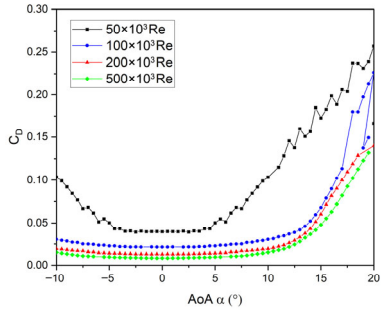

Figure 8. Drag Coefficient (C_D) vs. angle of attack (α) for the S1046 airfoil.

3.1.3. DU 06-W-200

Various studies show that airfoils with reduced curvature improve the performance of VAWTs in the windward section. However, they also have a negative impact on the leeward or downwind section. Maximum power can be obtained with a curvature of approximately 3%. The DU 06-W-200 airfoil was created specifically for use in VAWTs [19], and one inspiration for its development was the search for an airfoil with better aerodynamic and structural characteristics than the NACA 0018. Figure 9 shows the behavior of C_L vs. α for different *Re*, and a linear behavior is observed for values between 0° and 12° with *Re* greater than 100×10^3. However, as with the NACA 0021 profile, the curve for a $Re = 50 \times 10^3$ shows a sharp drop in aerodynamic performance at very low angles of attack. Figure 10 shows the C_D vs. α curves for this profile, where stable behavior is observed from −3° to 3° for $Re = 50 \times 10^3$, increasing abruptly from there. For *Re* values between 200×10^3 and 500×10^3, stability in C_D occurs at values from −5° to 10°.

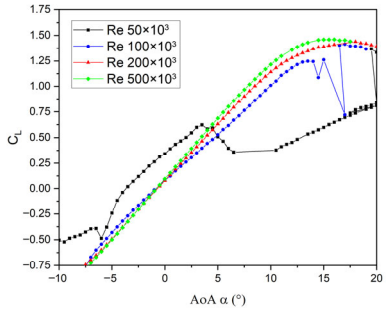

Figure 9. Lift coefficient (C_L) vs. angle of attack (α) for the DU 06-W-200 airfoil.

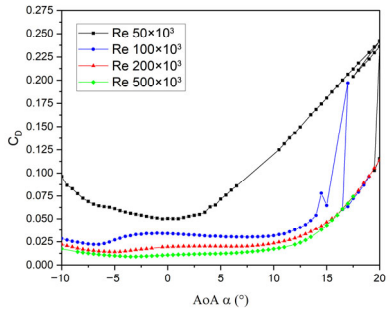

Figure 10. Drag coefficient (C_D) vs. angle of attack (α) for the DU 06-W-200 airfoil.

The behavior of the lift and drag coefficients has been shown for three profiles proposed for study. The next step is to evaluate the power coefficient *Cp* of the nine proposed airfoils shown in Figure 4.

3.2. Power Coefficient Evaluation

The power coefficient of nine airfoils was evaluated to select the most suitable for the wind conditions of the Yucatán Peninsula. Three tests were carried out at speeds of 4, 5, and 6 m/s. Figure 11 shows the C_p vs. *TSR* (Tip-Speed Ratio) curves corresponding to the nine airfoils analyzed at a wind speed of 4 m/s. The S1046 airfoil achieved the highest power coefficient (C_p = 0.45) at a *TSR* of 3.2. The DU 06-W-20 airfoil shows a C_p greater than 0.4 for a *TSR* of 2.8, the lowest of all the airfoils analyzed. However, its performance is inferior to that of the S1046 airfoil. The NACA 0021 airfoil performs similarly to the DU 06-W-20, with a maximum TSR of 3.3.

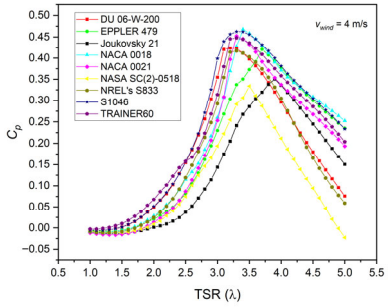

Figure 11. Power coefficient (C_p) vs. TSR (λ) for airfoils at 4 m/s.

Figure 12 shows the C_p vs. *TSR* curves for the nine airfoils analyzed at a wind speed of 5 m/s. The airfoils with the best aerodynamic performance are EPPLER 479, NACA 0018, and S1046, which have a maximum C_p of 0.52 for a *TSR* of 3.3. The NASA SC(2)-0518, meanwhile, shows the worst performance, with a maximum C_p of less than 0.45 at a *TSR* of 3.2.

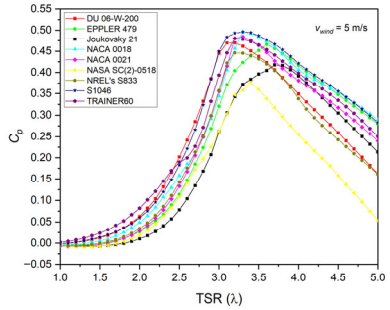

Figure 12. Power coefficient (C_p) vs. TSR (λ) for airfoils at 5 m/s.

Figure 13 shows the C_p vs. TSR curves for the nine airfoils analyzed at a wind speed of 6 m/s. The airfoils with the best performance are the same as in the 5 m/s test: EPPLER 479, NACA 0018, and S1046, which have a maximum C_p of 0.56 at a TSR of 3.3. The NASA SC (2)-0518 profile has the worst performance, with a maximum C_p of 0.50 at a TSR of 2.8.

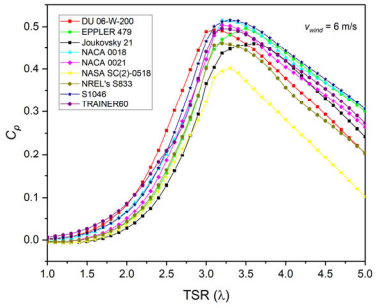

Figure 13. Power coefficient (C_p) vs. TSR (λ) for airfoils at 6 m/s.

All the airfoils studied show similar performance for average wind speeds of 5 and 6 m/s. However, for a wind speed of 4 m/s, the S1046 airfoil exhibits a higher C_p than every other airfoil studied. In all tests performed, the S1046 profile showed superior design, with the NACA 0018 showing similar performance, and was therefore chosen for use in the VAWT design.

3.3. Wind Turbine Design Parameters

The design parameters for the proposed vertical axis wind turbine must take into account low power generation in urban environments and low-wind-speed conditions (4–5 m/s). A cross-sectional area of 4 m^2 is therefore proposed, like those used in commercial devices with the same characteristics. This input parameter, together with the solidity (σ) and aspect ratio of the rotor ($A_r = H/R$), limits the dimensions of height (H), radius (R), and chord length (C) for the designed device. Preliminary tests using the QLLT or "Vortex" method indicate that the Re for a TSR of 3 and a wind speed of 4 m/s is in the range of 70×10^3, as shown in Figure 14. Therefore, the appropriate polars for the analysis are in the range of 100×10^3 Re.

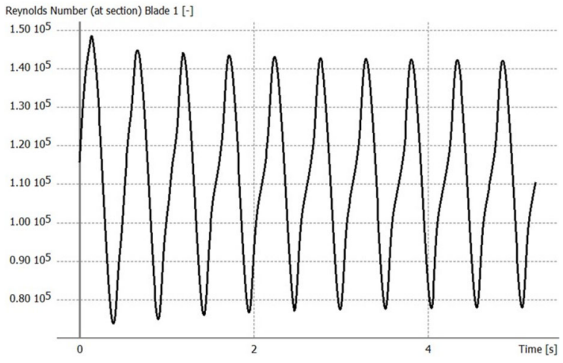

Figure 14. Reynolds variation, Re vs. time.

3.3.1. Qblade Configuration

Wind turbine analysis using the DMS method was performed in QBlade, where the polars had to be generated and the simulation parameters configured. The default configuration was used, activating the Tip Loss checkbox, which allows the inclusion of finite blade length in the calculations, as well as the Variable induction factors checkbox to execute the DMS method iterations for each azimuth position.

3.3.2. Rotor Aspect Analysis

A widely used parameter for VAWT design is the turbine aspect ratio (A_r), which is the ratio of blade height to rotor radius.

$$A_r = \frac{h}{R} \tag{11}$$

where H is the height of the blade and R is the rotor radius. The recommended values for A_r are between 2.6 and 3 (The optimal value is higher if structural stresses are ignored, i.e., if only the aerodynamic optimization of the blade is considered).

From the cross-sectional area of the rotor, the height H is defined as:

$$H = \frac{2}{R} \tag{12}$$

Substituting H into A_r yields an expression in terms of the rotor radius, R.

$$A_r = \frac{2}{R^2} \tag{13}$$

This can be expressed as:

$$R = \sqrt{\frac{2}{A_r}} \tag{14}$$

As previously mentioned, the recommended values for A_r should be between 2 and 3. Therefore, the maximum and minimum dimensions of the rotor radius can be expressed as:

$$R_{min} = \sqrt{\frac{2}{3}} \approx 0.816 \text{ m}$$

$$R_{min} = \sqrt{\frac{2}{2.6}} \approx 0.877 \text{ m}$$

3.4. Description of the Solidity Analysis

The solidity of a wind turbine is a parameter that quantifies the ratio of the area occupied by the blades to the total cross-sectional area. It can be defined as:

$$\sigma = \frac{NC}{R} \tag{15}$$

where N represents the number of blades, C is the chord length, and R is the rotor radius. Various authors indicate that the optimal solidity value for a VAWT lies between 0.2 and 0.3. From Equation (15), it is evident that varying the number of blades, chord length, or rotor radius results in a change in solidity. These variables also affect other parameters and have their own optimal value ranges. For example, the recommended number of blades is between 2 and 5, where it has been observed that a lower number of blades generates a higher power coefficient but has negative effects such as increased torque variation and reduced starting capability.

Rearranging Equation (15) gives:

$$C = \frac{R\sigma}{N} \tag{16}$$

This allows obtaining the chord length intervals for different numbers of blades. By substituting Equation (14) into Equation (16), the blade chord length can be expressed as a function of A_r, σ, and N as follows:

$$C = \frac{\sqrt{\frac{2}{A_r}}\sigma}{N} \tag{17}$$

Table 2 shows the minimum and maximum chord values according to the number of blades of the VAWT.

Table 2. Minimum and maximum chord values for different numbers of blades in the VAWT.

No. of Blades	C_{min}	C_{max}
2	$C_{min} = \frac{R_{min}\sigma_{min}}{2} = \frac{\sqrt{\frac{2}{3}}*0.2}{2} \approx 0.081$ m	$C_{max} = \frac{R_{max}\sigma_{max}}{2} = \frac{\sqrt{\frac{2}{2.6}}*0.3}{2} \approx 0.131$ m
3	$C_{min} = \frac{R_{min}\sigma_{min}}{2} = \frac{\sqrt{\frac{2}{3}}*0.2}{3} \approx 0.054$ m	$C_{max} = \frac{R_{max}\sigma_{max}}{2} = \frac{\sqrt{\frac{2}{2.6}}*0.3}{3} \approx 0.087$ m
4	$C_{min} = \frac{R_{min}\sigma_{min}}{2} = \frac{\sqrt{\frac{2}{3}}*0.2}{4} \approx 0.040$ m	$C_{max} = \frac{R_{max}\sigma_{max}}{2} = \frac{\sqrt{\frac{2}{2.6}}*0.3}{4} \approx 0.065$ m
5	$C_{min} = \frac{R_{min}\sigma_{min}}{2} = \frac{\sqrt{\frac{2}{3}}*0.2}{5} \approx 0.032$ m	$C_{max} = \frac{R_{max}\sigma_{max}}{2} = \frac{\sqrt{\frac{2}{2.6}}*0.3}{5} \approx 0.052$ m

These values will be used in the *DMS* simulation to determine the VAWT power coefficient based on the *TSR*.

3.5. Solidity Analysis of the VAWT

3.5.1. First Stage Simulation

Table 3 shows the parameters for configuring the VAWT geometry for the DMS simulations. There are eight simulations in total.

Table 3. Geometry settings for DMS simulation.

Number of Blades	Radius (m)	
	R_{min} = 0.81	R_{max} = 0.877
2	C = 0.081 m	C = 0.131 m
3	C = 0.054 m	C = 0.087 m
4	C = 0.040 m	C = 0.065 m
5	C = 0.032 m	C = 0.052 m

Figure 15 shows the power coefficient as a function of TSR (λ), showing a clear upward trend in the power coefficient as the number of blades decreases. 5-blade wind turbines have the lowest performance, with the A_r = 3 and σ = 0.2 configuration showing the worst performance, as it does not generate any power for any TSR value. This is largely due to the Reynolds at which it operates, since the chord of the blades is reduced with an increase in the number of blades to maintain solidity within the recommended range of values. Thus, when operating at lower *Re* (50,000 or less), the lift coefficient decreases considerably compared to wind turbines of the same solidity but with fewer blades.

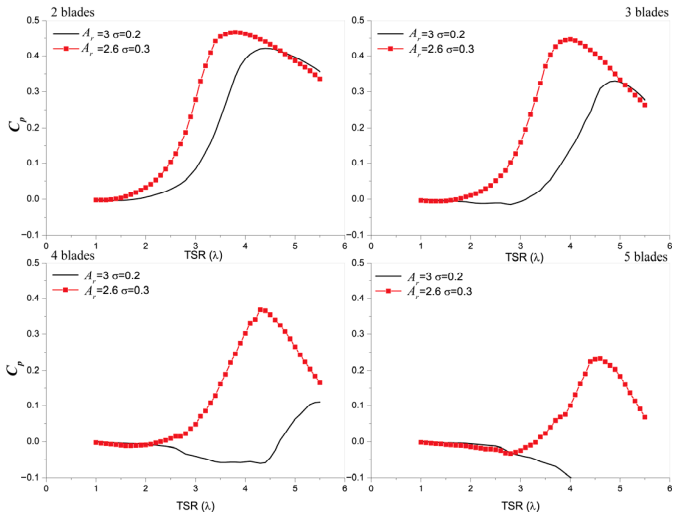

Figure 15. Power coefficient C_p vs. TSR (λ) for VAWTs with 2, 3, 4 and 5 blades.

As for the top-performing wind turbine, the observed tendency is towards fewer blades combined with greater solidity and low A_r as the optimal combination for higher C_p. The highest power coefficient obtained is approximately 0.47 for the wind turbine with two blades, with a solidity of 0.3 and an A_r of 2.6. The general trend observed in the aspect ratio is an increase in the power coefficient as the aspect ratio decreases. However, because this also coincides with the maximum solidity values, it is not entirely clear at this early stage whether the observed behavior is related. Figure 16 shows the power coefficient as a function of $TSR(\lambda)$ for the eight wind turbine configurations analyzed in the first stage. The observed tendency confirms the inverse relationship between the number of blades and the power coefficient. On the other hand, there is a clear difference between the two configurations analyzed, with the combination of lower aspect ratio and higher solidity generating higher maximum power coefficient values. The C_p results shown in Figure 15, for $N = 2$ and $N = 4$, are like those reported by [22] for a VAWT with a NACA 0021 airfoil for $N = 2$ ($C_p = 0.4$ and $\lambda = 5$) and $N = 4$ ($C_p = 0.5$ and $\lambda = 3.5$).

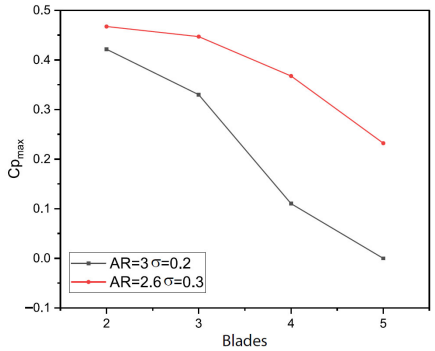

Figure 16. Maximum power coefficient $C_{p_{max}}$ as a function of the number of blades.

3.5.2. Second Stage Simulation

Previous results showed that wind turbines with fewer blades (2–3) perform better. Therefore, for the second stage of analysis, new configurations are proposed that take the following constraints into account:

- Area = 4 m^2
- Blades = 2–3
- Solidity σ = 0.200, 0.225, 0.25, 0.275 and 0.300
- Blade aspect ratio AR = 2.6, 2.7, 2.8, 2.9 and 3.0

These parameters coincide with the values recommended in the literature [3], as well as the configurations that have shown the best results (higher overall and maximum power coefficient) in previous analyses.

3.5.3. Two Blade VAWT

Five solidity values and five A_r values are proposed, resulting in 25 possible design combinations, two of which have already been evaluated in the previous stage. Table 4 shows the configurations of the 2-blade VAWT geometry that will be analyzed. Airfoil chord values were obtained using Equation (17).

Table 4. Chord values C (m) as a function of A_r and σ for a VAWT with N = 2.

A_r	Solidity				
	0.200	**0.225**	**0.250**	**0.275**	**0.300**
3	0.081	0.091	0.102	0.112	0.122
2.9	0.083	0.093	0.103	0.114	0.124
2.8	0.084	0.095	0.105	0.116	0.126
2.7	0.086	0.096	0.107	0.118	0.129
2.6	0.087	0.098	0.109	0.120	0.131

Figure 17 shows the C_p values as a function of λ. The results are organized for different A_r values, with each sub-graph showing the curves for different σ values. For any A_r value, the trend for σ is directly proportional to C_p, such that for all curves, the higher C_p values belong to the wind turbines with greater solidity. The λ values used to derive C_p range from 3 to 4.5, which is consistent with values obtained in similar designs [3].

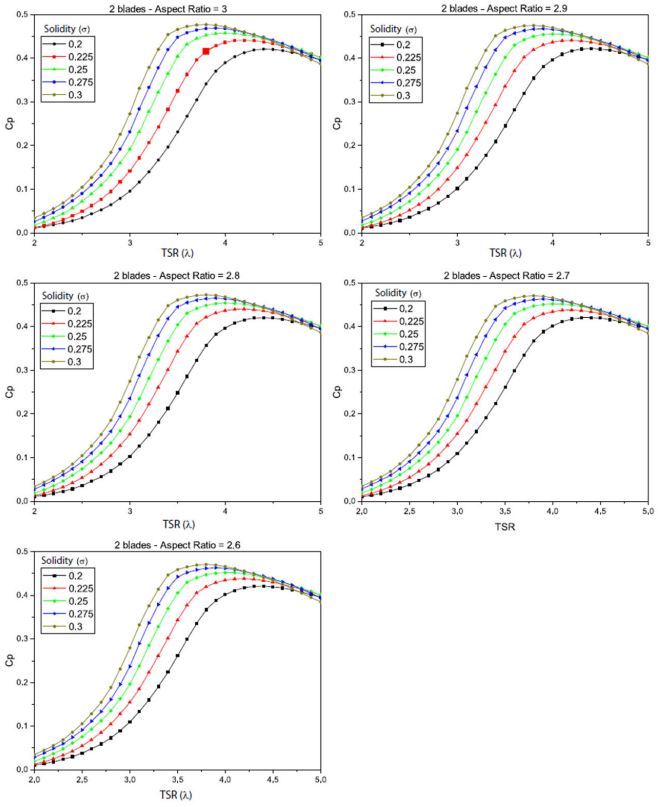

Figure 17. Power coefficient C_p as a function of TSR (λ) for a 2-blade VAWT.

The results also show that, for 2-bladed wind turbines, A_r has a minimal impact on the maximum power coefficient (within the range studied), with maximum variations of 2%. On the other hand, the impact of solidity is more pronounced, as seen in Figure 18, since increasing solidity drastically reduces the maximum power coefficient and shifts the maximum λ point to higher values.

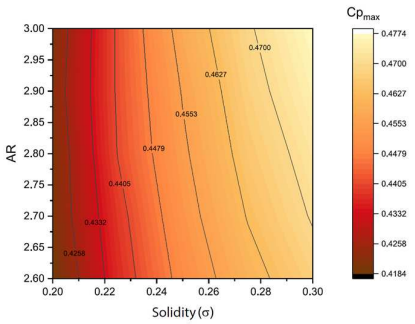

Figure 18. Maximum coefficient $C_{p_{max}}$ as a function of σ and A_r for a 2-blade VAWT.

Solidity is directly related to airfoil chord length. Thus, higher solidity values correspond to wind turbines with longer chord lengths, which generate higher *Re* values. Once again, it appears that *Re* has the greatest impact on the performance of the devices studied, which is common in small wind turbines.

Figure 18 shows the variation in the maximum power coefficient for the 25 three-bladed devices analyzed, arranged in a matrix. The *x*-axis represents solidity and the *y*-axis represents A_r. The lowest $C_{p_{max}}$ values are shown in red, while the highest are in yellow. The maximum power coefficient values vary between approximately 0.33 and 0.45. The general trend shows the best performing wind turbines to be those with greater solidity and lower A_r.

3.5.4. Three Blade VAWT

As in the previous section, five solidity values and five A_r values are proposed for this configuration, generating 25 combinations of proposed designs, two of which have already been evaluated in the previous stage. Table 5 shows the configurations of the 3-blade VAWT geometry to be analyzed.

Table 5. Chord values C (m) as a function of A_r and σ for a VAWT with N = 3.

A_r	Solidity				
	0.200	**0.225**	**0.250**	**0.275**	**0.300**
3	0.054	0.061	0.068	0.074	0.081
2.9	0.055	0.062	0.069	0.076	0.083
2.8	0.056	0.063	0.070	0.077	0.084
2.7	0.057	0.064	0.071	0.078	0.086
2.6	0.058	0.065	0.073	0.080	0.087

Figure 19 presents the power coefficient values as a function of λ. The results are again organized for different A_r values, where each sub-graph shows the curves for different σ values. For any A_r value, the trend for solidity is again directly proportional to the power coefficient. For all curves, the highest power coefficient values belong to wind turbines with higher σ. The values of λ at which the maximum power coefficient is obtained vary between 3.5 and 5, which coincides with values obtained in similar designs [3]. The results

also show that, for 3-bladed wind turbines, the aspect ratio has an inversely proportional relationship with the maximum power coefficient (within the range studied). On the other hand, the impact of solidity is more pronounced, as seen in Figure 19, since increasing solidity drastically reduces the maximum power coefficient and shifts the maximum λ point to higher values.

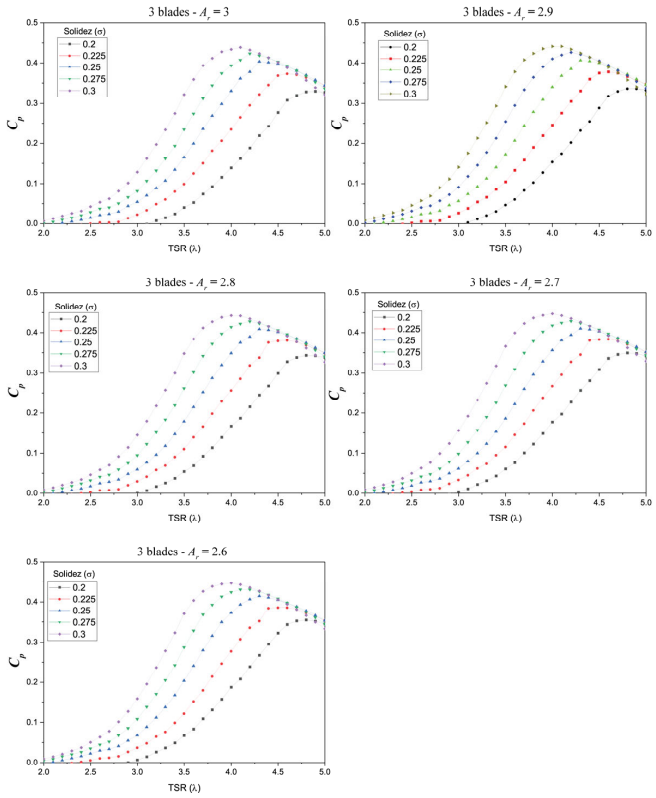

Figure 19. Power coefficient C_p as a function of TSR (λ) for a 3-blade VAWT.

In terms of solidity, the analysis carried out for 2-blade wind turbines appears to be valid for 3-blade turbines. Figure 20 shows the variation in the maximum power coefficient for the 25 three-bladed devices analyzed, arranged in a matrix. The x-axis represents solidity and the y-axis represents A_r. The lowest $C_{p_{max}}$ values are shown in red, while the highest values are in yellow. The maximum power coefficient values vary between approximately 0.33 and 0.45. The general trend shows that the best-performing wind turbines are those with greater solidity and lower A_r.

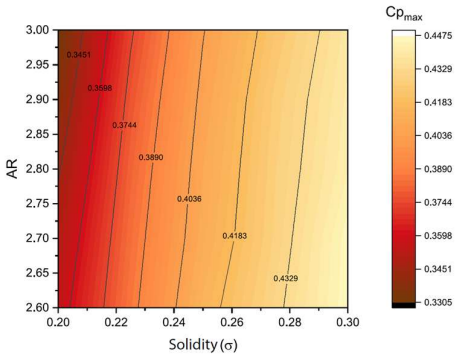

Figure 20. Power coefficient C_p as a function of solidity (σ) and A_r for a 3-blade VAWT.

4. Analysis of Results and Discussion

This study evaluated nine aerodynamic profiles using DMS and QLLT models to identify which would maximize the power coefficient (C_p) of a low-power VAWT designed for wind conditions on the Yucatán Peninsula. The results using Qblade software showed that the S1046 and NACA 0018 airfoils achieved C_p values greater than 0.45 in tests at 5 m/s and 6 m/s, with both being practically equivalent in aerodynamic performance, suggesting that symmetrical airfoils perform better in VAWTs. This superiority is observed both in the optimal TSR range (3–3.3) and in the stability of the lift and drag curves against Reynolds variations in the range 100×10^3 to 200×10^3.

Comparison of the DMS and QLLT models revealed that, although DMS overestimates the optimal *TSR* ($\lambda \approx 4$) relative to QLLT ($\lambda \approx 3.75$), both methods agree on the general trend of the C_p vs. λ curve, see Figure 21. The QLLT method provides a more conservative and realistic prediction of the maximum C_p (0.48), due to is a nonlinear lifting-line/free-vortex-wake approach that resolves 3D bound vorticity and wake interactions, using more computing resources. Therefore, the QLLT model could offer more reliable estimates of actual performance.

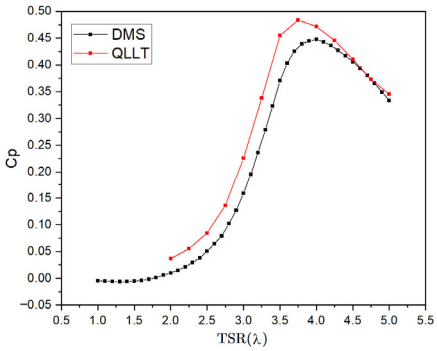

Figure 21. Power coefficient C_p vs. TSR (λ) of the selected VAWT (σ = 0.3, A_r = 2.6 and N = 3).

Analysis of the rotor geometry showed that the configuration with fewer blades tends to increase the maximum C_p. In the first stage, two-bladed VAWTs showed a maximum C_p of approximately 0.47, compared to 0.45 for three-bladed VAWTs, considering A_r = 2.6 and σ = 0.3. However, in the second stage of optimization, when varying A_r (2.6–3.0) and σ (0.2–0.3), it was observed that the influence of solidity exceeds that of A_r. An increase in σ improves C_p to a certain extent, due to the associated increase in the *Re*, but it also shifts the optimal *TSR* to higher values (4–4.5), which could limit operability in the lower winds typical of urban areas.

On the other hand, the blade aspect ratio (A_r) showed different behaviors depending on the number of blades. For two-bladed VAWTs, the variation in A_r in the range studied had little effect on the maximum C_p ($\pm$2%), suggesting that in dual-blade designs, the priority lies in achieving a high *Re* rather than optimizing A_r. In tri-blade designs, however, a lower A_r correlated with a significant increase in C_p (up to 0.45), indicating that the interaction between induction and edge losses is more sensitive to height in tri-blade turbines. The final selection, A_r = 2.6, and σ = 0.3 reflects a compromise between energy performance, and torque produced at low TSRs. Although two-bladed VAWTs offer a slight energy benefit, their start-up capacity is reduced and their behavior in turbulent conditions is less predictable, which could lead to higher dynamic loads on the tower (Figures 15 and 16). Likewise, the economic and manufacturing evaluation supports the choice of three blades: the difference in materials (one additional blade) is offset by a reduction in external start-up system requirements and maintenance costs, since a tri-blade configuration better distributes cyclic loads and produces less vibration compared to a dual-

blade design. To evaluate the self-starting between 2- and 3-blade VAWT's simulation at 3 m/s wind velocity on DMS QBlade analysis module was conducted. Figure 22 shows that although the 2-blade VAWT exhibits higher static torque peaks, the torque obtained during one revolution is lower than in a 3-blade VAWT, which justifies its selection. Although the static torque results are adequate for self-starting, there is a possibility that an external starting system may be required, since QBlade does not consider rotor inertia in its torque calculation. Similar torque values were reported by [23] for a VAWT with R = 0.175 m, C = 0.071 m, σ = 1.15, AR = 1, and N = 3.

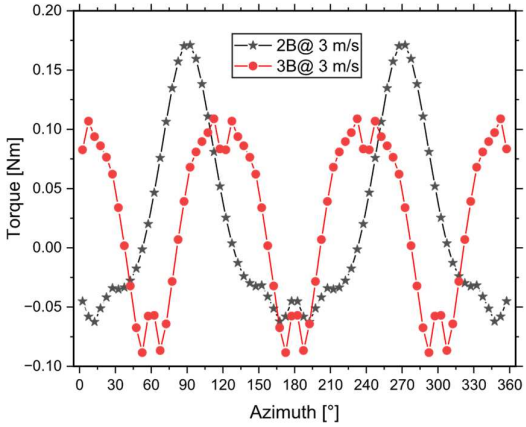

Figure 22. Static torque vs. Azimuth for VAWT's with 2 and 3 blades.

Results of the QLLT analysis with QBlade confirm the viability of using open-source software for the parametric design of VAWTs, as it adequately reproduces the trends observed in classic experimental studies [15] and coincides with recent findings in the literature on the optimization of profiles and geometries for low power. This demonstrates that open-source tools can meet the research and development needs of small-scale wind devices, especially in academic or low-budget contexts.

The C_p values with the selected wind turbine (S1046, N = 3, σ = 0.3) agree with those reported by [9], who developed a computational fluid dynamics numerical model to evaluate the aerodynamic performance of a Darrieus-type VAWT with N = 3, σ = 0.2–0.8, wind velocity = 9 m/s, λ = 0.5–3, and variable pitch. The C_p values obtained ranged from 0.38 to 0.44 for solidities of 0.2 and 0.8, respectively. On the other hand, ref. [24] report an experimental study on the effect of solidity on aerodynamic forces in a VAWT, depending on the number of blades. They report maximum C_p values ranging from 0.18 to 0.21, for λ = 1.3 to 2.2. McNaugthon et al. [25] have investigated to model the turbulence in VAWTs at low Reynolds numbers. The method used by McNaugthon consisted of two-dimensional computational fluid dynamics study using the SST turbulence model of a VAWT with N = 3, NACA 0018 airfoil profile, and C = 3.2 cm at a wind speed of 2.3 m/s. These results showed a C_p greater than 0.5 for a λ = 2 and an azimuth of 0 and 180°.

To provide a more comprehensive assessment of the wind turbine's performance, a multivariate analysis was conducted across a range of wind velocities. Figure 23 illustrates the relationship between generated power and rotational speed for different mean wind velocities. The operating points associated with maximum power output are highlighted, and their estimated values are indicated in the figure. All results were obtained using the DMS model. At the representative mean wind velocity estimated for the Yucatán Peninsula, the rotor achieves a maximum output of approximately 136 W at a rotational speed of 220 rpm. Under higher-mean-wind conditions—characteristic of specific locations within the region—the VAWT demonstrates a significantly enhanced power extraction capability. For example, at a mean wind speed of 9 m/s, the predicted power output

reaches approximately 932 W. Nevertheless, as such wind conditions are atypical for the area, this result is reported exclusively for characterization purposes.

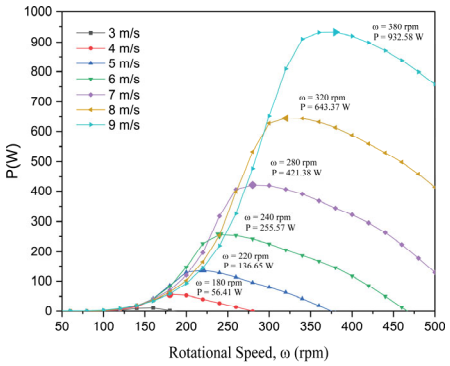

Figure 23. Power variation as a function or rotational speed for different average wind velocities.

5. Conclusions

The aerodynamic and parametric analysis demonstrates that the S1046 and NACA 0018 airfoils are optimal for low-power VAWTs under the prevailing wind conditions of the Yucatán Peninsula. Both airfoils achieve maximum power coefficients close to 0.51–0.52 at a wind speed of 6 m/s and an optimal tip-speed ratio (TSR) of around 3, while also exhibiting stable performance over a wide Reynolds range (100×10^3 to 200×10^3). This stability ensures that local wind variations, typical of urban and coastal environments, do not significantly compromise the turbine's energy performance.

The comparison between the wing design methods (DMS) and the quasi-linear shear layer theory (QLLT) revealed that, while the DMS model tends to slightly overestimate both the optimal TSR (placing it around 4) and the maximum power coefficient, the QLLT offers more conservative predictions that are closer to actual behavior. In particular, QLLT places the maximum C_p at approximately 0.48 at a TSR of 3.75, effectively incorporating the structural losses associated with the support arms. Therefore, QLLT is recommended as the primary method for the preliminary design of low-power VAWTs, complemented by specific validations using DMS or open-source CFD tools.

As regards geometric rotor configuration, a three-bladed turbine with an aspect ratio (A_r) of 2.6 and a solidity (σ) of 0.3 was found to be an optimal compromise between aerodynamic efficiency, self-starting capacity, and structural stability. Although two-blade designs have a slight advantage in terms of maximum power coefficient (up to 0.47), their low starting torque make them less suitable for urban or residential applications where winds are often intermittent and low in intensity.

Another relevant finding is that the aspect ratio has a different effect depending on the number of blades; in dual-blade designs, varying the A_r in the range studied barely modifies the maximum C_p, while in tri-blade structures, a lower A_r slightly improves aerodynamic interaction, increasing overall performance. However, solidity proved to be the parameter with the greatest influence on performance, so its careful adjustment is more critical than modifying the height of the blade.

Open-source tools like QBlade were successfully validated for parametric design and aerodynamic optimization of low-power VAWTs. The results obtained with QBlade satisfactorily reproduce the trends observed in historical experiments and contemporary studies, demonstrating that open-source tools are sufficiently robust for academic and local development projects with limited budgets, reducing computational costs in comparison to computational fluid dynamics simulations during the design process. This enables universities and research institutes to develop prototypes and conduct field tests without relying on expensive commercial licenses.

Finally, for the design and implementation of medium-scale wind turbines in the Yucatán Peninsula, manufacturing blades with an S1046 profile, a constant solidity of 0.3 and an A_r of 2.6 is recommended, as well as operating the turbine at an approximate *TSR* of 3.75. Field tests are also recommended to validate performance under real conditions, as is a detailed structural analysis of the mounting arms to ensure durability under cyclic loads. Future research could include multi-objective optimizations that integrate cost, life cycle, and manufacturability criteria, as well as the exploration of advanced materials for blades that reduce weight and increase corrosion resistance in marine environments. This work thus lays the foundation for the development of efficient and economical low-power VAWTs perfectly adapted to local wind resources.

Author Contributions: F.D.-C. was responsible for the methodology, software implementation, formal analysis, validation, and visualization. J.O.A. contributed to the conceptualization of the study, supervised the research, prepared the original draft of the manuscript, and managed the project. N.R.-H. contributed to the methodology and the development of the QLLT and DMS models, as well as to validation. E.S. contributed to the editing, critical revision of the manuscript, and visualization. O.A.J. contributed to the revision of the manuscript, the interpretation of the results, and supervision. All authors have read and agreed to the published version of the manuscript.

Funding: This research received no external funding.

Institutional Review Board Statement: Not applicable.

Informed Consent Statement: Not applicable.

Data Availability Statement: The data generated in the course of this research may be requested by email from the corresponding author.

Acknowledgments: F. Díaz-Canul would like to thank the National Council for Science and Technology (Government of Mexico) for the postgraduate scholarship awarded, and thanks the Division of Science, Engineering, and Technology at the Autonomous University of the State of Quintana Roo for the facilities provided for the development of his master's thesis in Mechatronics. The authors gratefully acknowledge the support of the Autonomous University of the State of Quintana Roo (UQRoo) in this publication.

Conflicts of Interest: The authors declare no potential conflict of interests.

Abbreviations

The following abbreviations are used in this manuscript:

A	Rotor swept area (m^2)
AR	Aspect ratio (H/R)
C	Airfoil chord (m)
C_D	Drag coefficient
C_L	Lift Coefficient
C_p	Power coefficient
D	Rotor diameter (m)
DMS	Double Multiple Stream tube
F_D	Drag force (N)
F_L	Lift force (N)
F_n	Normal force (N)
F_t	Tangential force (N)
H	Rotor height (m)
N	Number of blades
P	VAWT Power
QLLT	Qblade Lifting Line Theory

R	Rotor radius (m)
T	VAWT torque (N m)
v_c	Chord velocity (m/s)
v_n	Normal velocity (m/s)
v_a	Axial velocity (m/s)
W	Relative airflow velocity (m/s)
VAWT	Vertical Axis Wind Turbine
Greeks	
α	Angle of attack (°)
λ	Tip Speed Ratio (TSR)
σ	Solidity
θ	Azimuth angle (°)
ϕ	Height/Diameter ratio (H/D)
ω	Rotational speed (rpm)

References

1. Firdaus, R.; Kiwata, T.; Kono, T.; Nagao, K. Numerical and experimental studies of a small vertical-axis wind turbine with variable-pitch straight blades. *J. Fluid Sci. Technol.* **2015**, *10*, JFST0001. [CrossRef]
2. Bianchini, A.; Ferrara, G.; Ferrari, L. Design guidelines for H-Darrieus wind turbines: Optimization of the annual energy yield. *Energy Convers. Manag.* **2015**, *89*, 690–707. [CrossRef]
3. Hand, B.; Kelly, G.; Cashman, A. Aerodynamic design and performance parameters of a lift-type vertical axis wind turbine: A comprehensive review. *Renew. Sustain. Energy Rev.* **2021**, *139*, 110699. [CrossRef]
4. Miliket, T.A.; Ageze, M.B.; Tigabu, M.T. Aerodynamic performance enhancement and computational methods for H-Darrieus vertical axis wind turbines: Review. *Int. J. Green Energy* **2022**, *19*, 1428–1465. [CrossRef]
5. Islam, M.; Ting, D.S.-K.; Fartaj, A. Design of a Special-Purpose Airfoil for Smaller-Capacity Straight-Bladed VAWT. *Wind Eng.* **2007**, *31*, 401–424. [CrossRef]
6. Tirandaz, M.R.; Rezaeiha, A. Effect of airfoil shape on power performance of vertical axis wind turbines in dynamic stall: Symmetric Airfoils. *Renew. Energy* **2021**, *173*, 422–441. [CrossRef]
7. Davari, H.S.; Botez, R.M.; Davari, M.S.; Chowdhury, H. Blade height impact on self-starting torque for Darrieus vertical axis wind turbines. *Energy Convers. Manag. X* **2024**, *24*, 100814. [CrossRef]
8. Rezaeiha, A.; Montazeri, H.; Blocken, B. Towards optimal aerodynamic design of vertical axis wind turbines: Impact of solidity and number of blades. *Energy* **2018**, *165*, 1129–1148. [CrossRef]
9. Sagharichi, A.; Zamani, M.; Ghasemi, A. Effect of solidity on the performance of variable-pitch vertical axis wind turbine. *Energy* **2018**, *161*, 753–775. [CrossRef]
10. Miller, M.A.; Duvvuri, S.; Hultmark, M. Solidity effects on the performance of vertical-axis wind turbines. *Flow* **2021**, *1*, E9. [CrossRef]
11. Chávez, S. Diseño de un Microaerogenerador de Eje Vertical. Bachelor's Thesis, Universidad Nacional Autónoma de México, Ciudad Universitaria, Mexico, 2010.
12. Hernández, M.R.; de la Torre, J.; Contreras, J.L.N.; Guzman, G.R.; Martínez, J.R.; Ruedas, F.B. Diseño y construcción de aerogenerador de eje horizontal de 1 kW. *Rev. Difusión Científica Ing. Tecnol.* **2012**, *5*, 51–59.
13. García, L.; Treviño, A.; Lara, D.; Romero, G.; Ramírez, L.; Romero, L. Desarrollo de una plataforma experimental para una nueva configuración de un aerogenerador de eje vertical. In Proceedings of the SOMI Congreso de Instrumentacion XXIX Edicion, Puerto Vallarta, Mexico, 29–31 October 2014.
14. Nugraha, A.D.; Garingging, R.A.; Wiranata, A.; Sitanggang, A.C.; Supriyanto, E. Comparison of "Rose, Aeroleaf, and Tulip" vertical axis wind turbines (VAWTs) and their characteristics for alternative electricity generation in urban and rural areas. *Results Eng.* **2025**, *25*, 103885. [CrossRef]
15. Blackwell, B.F.; Sheldahl, R.E.; Feltz, L.V. *Wind Tunnel Performance Data for the Darrieus Wind Turbine with NACA 0012 Blades*; Sandia Laboratories Energy Report: Albuquerque, NM, USA, 1976.
16. Díaz-Canul, F.; Rosado-Hau, N.; Aguilar, J.O.; Becerra-Núñez, G.; Jaramillo, O.A. Diseño de un rotor Darrieus tipo Phi para aerogeneradores de baja potencia. *Ing. Investig. Tecnol.* **2024**, *25*, 1–12. [CrossRef]
17. Islam, M.; Ting, D.S.-K.; Fartaj, A. Aerodynamic models for Darrieus-type straight-bladed vertical axis wind turbines. *Renew. Sustain. Energy Rev.* **2008**, *12*, 1087–1109. [CrossRef]
18. Tjiu, W.; Marnoto, T.; Mat, S.; Ruslan, M.H.; Sopian, K. Darrieus vertical axis wind turbine for power generation I: Assessment of Darrieus VAWT configurations. *Renew. Energy* **2015**, *75*, 50–67. [CrossRef]

19. Claessens, M.C. The Design and Testing of Airfoils for Application in Small Vertical Axis Wind Turbines. Master's Thesis, Delft University of Technology, Delft, The Netherlands, 2006.
20. Ferreira, C.S.; Geurts, B. Aerofoil optimization for vertical-axis wind turbines. *Wind Energy* **2015**, *18*, 1371–1385. [CrossRef]
21. Mohamed, M.H. Performance investigation of H-rotor Darrieus turbine with new airfoil shapes. *Energy* **2012**, *47*, 522–530. [CrossRef]
22. Mahmood, Y.H.; Badah, M.R. Design vertical axis wind turbine rotorblade and simulation in (DMS) approach by QBlade software. *AIP Conf. Proc.* **2023**, *2593*, 020001. [CrossRef]
23. Davari, H.S.; Botez, R.M.; Davari, M.S.; Chowdhury, H.; Hosseinzadeh, H. Numerical and experimental investigation of Darrieus vertical axis wind. *Results Eng.* **2024**, *24*, 103240. [CrossRef]
24. McNaugthon, J.; Billard, F.; Revell, A. Turbulence modelling of low Reynolds number flow effects around a vertical turbine at a range of tip-speed ratios. *J. Fluidos Structires* **2014**, *47*, 121–138. [CrossRef]
25. Li, Q.; Maeda, T.; Kamada, Y.; Murata, J.; Shimizu, K.; Ogasawara, T.; Nakai, A.; Kasuya, T. Effect of solidity on aerodynamic forces around straight-bladed vertical axis wind turbine by wind tunnel experiments (depending on number of blades). *Renew. Energy* **2016**, *96*, 928–939.